Volume 15, Issue 3, 152537 (1-15)

Iranian Journal of Catalysis (IJC)

https://doi.org/10.57647/j.ijc.2025.1503.37

Fe_3O_4@3-Aminopropyltriethoxysilane-SO_3H: A greener catalyst for one-pot synthesis of pyranopyrimidine derivatives

Raju Shekhanavar, Aravind Kamath, Kantharaju Kamanna*

Department of Chemistry, Rani Channamma University, Belagavi, P-B, NH-4-591156, India.

***Corresponding author:** kk@rcub.ac.in

Original Research

Received:
4 March 2025
Revised:
6 June 2025
Accepted:
10 July 2025
Published online:
26 July 2025
Published in issue:
30 September 2025

Abstract:

The present work describes the eco-friendly preparation of magnetic nanoparticles Fe_3O_4 (MNPs) using Water Extract of Lemon Fruit Shell Ash (WELFSA) as a greener agro-waste solvent medium and further functionalized with 3-aminopropyltriethoxysilane and -SO_3H. The prepared heterogeneous Lewis acid was explored for one-pot synthesis of pyrano[2, 3-*d*]pyrimidine derivatives using aromatic aldehyde, ethyl cyanoacetate, and barbituric or thiobarbituric acid, accelerated by microwave irradiation in ethanol as a co-solvent. The reaction is optimized by various methods such as magnetic stirring, ultrasound, mechanochemical, and microwave irradiation, but the microwave irradiation method gives excellent product isolation with a faster rate and a high yield of $82-92\%$ with high purity. The advantages of the present approach are chemical-free, no hazardous solvents, and considered as an eco-friendly protocol for the synthesis of pyrano[2, 3-*d*]pyrimidine derivatives. The final product isolated is recrystallized in ethanol and characterized by FT-IR, ^{1}H-, ^{13}C-NMR, and LC-MS spectrometry. Further, some of the selected pyrano[2, 3-*d*]pyrimidine derivatives (4a, 4d, 4f, 4m, 4o, and 4r) are subjected to anti-microbial activity studies. The tested derivatives show anti-microbial activity comparable to the activities of reference antimicrobials.

Keywords: Green chemistry; Pyrano[2, 3-*d*]pyrimidine; APTES; Microwave irradiation; Anti-microbial

1. Introduction

Heterocyclic compounds have been identified as a predominant stream in organic chemistry [1]. Heterocycles are ubiquitous in nearly all branches of chemistry, and they are being successfully applied in biology, pharmacology [2], optics [3], material sciences [4], and numerous other fields of interest [5]. The heterocyclic family consists of various natural drugs like papaverine, theobromine, quinine, emetine, theophylline, atropine, procaine, codeine, reserpine, and morphine [6, 7]. Heterocycles have also been prepared to form stable metal complexes with different metal ions, which have indeed gained great biological significance [8]. Over the past decades, a sustainable and promising application has been expanded in numerous heterocycles owing to their broad spectrum of significance, for example, in the field of medicinal chemistry, drug discovery, and natural product synthesis, as well as the preparation of a diverse range of advanced materials [9]. Among various heterocycles, pyrano-pyrimidine heterocycles show an interesting range of biological functions. It is a six-membered unsaturated N-atom heterocycle consisting of pyran fused with pyrimidine rings, with an oxo-functionality at the eighth position and imide functionality at the first and third positions [10]. The work at hand discusses facile and efficient synthesis of these essential pyrano-pyrimidines, and assesses these compounds to find if any anti-bacterial/anti-fungal activity. Pyrano pyrimidines are aromatic heterocyclic compounds obtained by the uniting of 2N-atoms present on positions 1st & 3rd of the 6-membered ring of benzene and pyridine [11]. In the past century, pyrimidine-containing heterocycles have been widely investigated due to their biologically active properties [12]. These pyrimidine-based scaffolds displayed exemplary antibacterial, antitumor, anticonvulsant, cardiotonic, anti-inflammatory, anticancer, antiplasmodial, antihypertensive, antibronchitic, antifungal, and analgesic activities [13]. Due to its wide range of biological

activities, researchers have explored numerous synthetic routes for this heterocyclic motif [14]. Numerous synthetic routes for the synthesis of pyrano[2, 3-*d*]pyrimidine derivatives by the condensation reaction of benzaldehyde (1), ethyl cyanoacetate (2), and barbituric acid or thiobarbituric acid (3) in the presence of catalysts such as iron ore pellet [15], nano-sawdust-OSO_3H [16], Mn/ZrO_2 [17], cellulose-based nanocomposite [18], Fe_3O_4@SiO_2@$(CH_2)_3$-Urea-SO_3H/HCl [19], $ZnFe_2O_4$ nanoparticles [20], nickel iron oxide NPs [21], Fe_3O_4@MOF (Fe) NC [22], LDH@(3-chloropropyl)trimethoxysilane@N1, N4-*bis*(4,6-diamino-1,3,5-triazin-2-yl) benzene-1,4-disulfonamide@Cu [23], trimetallic multi-walled carbon nanotubes [24] have been reported. Herein we have demonstrated the one-pot synthesis of three-component reaction of pyrano[2, 3-*d*]pyrimidine derivatives based upon the model reaction of benzaldehyde (1), ethyl cyanoacetate (2), and barbituric acid or thiobarbituric acid (3) to give the title product. The reaction is catalyzed by Fe_3O_4@3-aminopropyltriethoxysilane-SO_3H (Fe_3O_4@APTES-SO_3H)and ethanol solvent under custom-made Microwave Irradiation (MWI). In this aspect, there are environmental-related challenges about the replacement with an aqueous phase instead of hazardous organic solvents for the green chemistry protocol, and chemists in recent years are focusing on it. We report herein the use of functionalized iron oxide as an efficient reusable catalyst for the synthesis of pyrano[2, 3-*d*]pyrimidine derivatives in a simple and recyclable route, and isolated high yield product.

2. Experimental

All chemicals were purchased from sd-fine and Avra. ^{1}H- and ^{13}C-NMR spectra were measured on a spectrometer at 400 MHz and 100 MHz, respectively, in DMSO-d_6. Fourier transform infrared (FT-IR) spectra were obtained using a Shimadzu 435-U-04 FT spectrophotometer from KBr pellets. Melting points were recorded on open capillary tubes and are uncorrected.

2.1 Preparation of extracts of lemon peel water

The lemon peel was obtained from a local fruit market, Belagavi, India. The outer shell was removed and washed with tap water in order to remove physical impurities on the surface. The obtained dry material was sun-dried and heated on a Bunsen burner to change the lemon peel into ash. Weighed 10 g of the resulting ash and dispersed in 100 mL double-distilled (dd) water and stirred for 1 h at room temperature. The precipitate was filtered, and the light brown-colour filtrate was named Water Extract of Lemon Fruit Shell Ash (WELFSA), and was directly used for the preparation of MNPs [25].

2.2 Preparation of Fe_3O_4 using WELFSA

To 3 g of $FeSO_4{\cdot}7H_2O$ in 50 mL of double-distilled water and 3 g of $FeCl_3{\cdot}6H_2O$ dissolved in a 100 mL beaker, 10 mL of WELFSA was added to it. The suspension was heated to 85 °C for approximately 45 min while stirring, and then allowed to cool to room temperature, and 2N NaOH solution was added drop-wise until a black precipitate appeared. The black precipitate was pulled out using a strong magnet and washed $2-3$ times with dd water and ethanol after the end of the reaction. The residue obtained was dried and calcinated to 400 °C for about 4 h in a muffle furnace, and stored in a desiccator in an air-tight container for further use.

2.3 Synthesis of Fe_3O_4@APTES

The prepared Fe_3O_4 MNPs (2.0 g) were dispersed in H_2O/EtOH (1:1) solution, taken in a 250 mL RB flask, followed by sonication for 45 min. Then, 3-aminopropyl triethoxysilane (2.5 mL) was added to this, and then mechanically agitated under a nitrogen atmosphere at 45 °C for 5 h, and then held externally by a strong magnet. To this, dd water was added (3 times) and sonicated, finally washed with water, followed by rectified spirit, and then decanted. The resulting product was dried at room temperature under vacuum, and stored in an air-tight container.

2.4 Preparation of Fe_3O_4@APTES-SO_3H

The above prepared Fe_3O_4@APTES (500 mg) was dispersed in dry dichloromethane (DCM), 3 mL, in an ultrasonic bath for 30 min, to which dropwise addition of chlorosulfonic acid (0.6 mL) was done over the period of 30 min at rt. During the reaction, the evolved HCl gas was taken out through the reaction vessel and bubbled into an external container filled with 2N NaOH solution. After stirring an additional 50 min at rt, the functionalized MNPs were magnetically separated and washed four times with dry DCM to remove excess acid before being dried in a hot air oven at 60 °C and stored in a desiccator till use.

2.5 Synthesis of 5-amino-6-hydroxy pyrano[2, 3-*d*]pyrimidine

Reactants aromatic aldehyde (1) (1 mmol), ethyl cyanoacetate (2) (1 mmol), barbituric or thiobarbituric acid (3) (1 mmol), 2 mL of ethanol and 10 mg of Fe_3O_4@APTES-SO_3H catalyst were placed in RB flask and irradiated with MW (300 W) equipped with magnetic stirring facility and reflux condenser. The thin layer chromatography (TLC) was used to monitor reaction and after completion of the reaction, hot EtOH was added (5 mL) followed by the separation of used catalysts using external magnet, decanting the reaction mixture, and concentrated to reduce solvent, cooled in ice water to give product isolation, which was chromatographically pure and excellent yield.

2.6 Solid acid titration

The acid functionalized sulfonic acid group (Fe_3O_4@APTES-SO_3H) was titrated by the common acid-base titration method. Briefly, 30 mg of the acid catalyst was taken in 50 mL of (0.01 M) NaOH in a conical flask (100 mL) kept at rt for about 3 h. Then the catalyst was filtered by magnetic rotator and washed with dd water (5 mL) for two times. After that, the filtrate was titrated to neutrality using a 0.01 M HCl solution using phenolphthalein indicator. The total acid group on Fe_3O_4@APTES MNPs, and in turn the number of Silica functionalized sulphonic acid (APTES-SO_3H), was found to be 0.45 mmol/g.

2.7 Some selected spectral data of synthesized derivatives

2.7.1 Ethyl-7-amino-2, 4-dioxo-5-phenyl-2, 3, 4, 5-tetrahydro-1H-pyrano[2, 3-*d*]pyrimidine-6-carboxylate (4a)

White powder; Yield: 96%; m.p.: 209 °C; FT-IR (cm^{-1}): 3206.3, 3134.3 (NH_2), 2954.4 (CH), 1702.2 (C=O), 1497.6 (C=C); ^{1}H-NMR δ (ppm): 2.04 – 2.10 (t, CH_3, 3H), 2.24 – 2.49 (q, CH_2, 2H), 4.50 (s, CH, 1H), 7.07 – 7.22 (m, 8H, Ar-H), 7.55 (s, 1H, Ar-H); ^{13}C NMR δ (ppm): 14.68, 26.94, 29.12, 32.35, 33.73, 39.58, 40.63, 59.45, 78.32, 116.04, 126.27, 128.16, 146.83, 159.62, 162.60, 168.46, 196.27ppm. LCMS: m/z (Cald.) $C_{16}H_{15}N_3O_5$ = 329.1158 $[M]^+$; m/z (Obs.) = 329.10.

2.7.2 7-Amino-5-(4-methoxyphenyl)-2, 4-dioxo-1, 3, 4, 5-tetrahydro-2H-pyrano[2, 3-*d*]pyrimidine-6-carboxylate (4b)

White powder; Yield: 94%; m.p.: 293 °C; FT-IR (cm^{-1}): 3913.92, 3193.93(NH_2), 3028.09(CH), 1713.95 (C=O), 1651.23 (C=C); ^{1}H-NMR δ(ppm): δ 1.31 – 1.34 (t, CH_3, 3H), 2.50 – 2.55 (q, CH_2, 2H), 4.64 (s, CH, 1H), 7.20 – 7.58 (m, 8H, Ar-H); ^{13}C NMR δ(ppm): 14.61, 28.27, 31.72, 39.80, 40.84, 47.03, 61.90, 92.52, 112.16, 115.41, 118.78, 127.50, 134.26, 134.26, 148.70, 154.19 ppm. LCMS: m/z (Cald.) $C_{16}H_{14}ClN_3O_5$ = 363.06 $[M]^+$; m/z (Obs.) = 363.75.

2.7.3 Ethyl-7-amino-5-(furan-2-yl)-4-oxo-2-thioxo-2, 3, 4, 5-tetrahydro-1H-pyrano[2, 3-*d*]pyrimidine-6-carboxylate (4c)

Brown powder; Yield: 96%; m.p.: 234 °C; FT-IR (cm^{-1}): 3431.26, (NH_2), 3089.45(CH), 1738.78(C=O), 1699.21(C=O), 1470.43 (C=S); ^{1}H-NMR δ (ppm): 2.06 – 2.10 (t, CH_3, 3H), 2.20 – 2.36 (q, CH_2, 2H), 3.92 – 3.94 (m, CH, 1H), 7.36 – 8.20 (m, 8H, Ar-H); ^{13}C NMR δ (ppm): 14.83, 26.77, 27.24, 29.15, 32.35, 40.62, 75.46, 104.98, 113.27, 141.30, 168.31, 196.09 ppm; LCMS: m/z (Cald.) $C_{16}H_{14}BrN_3O_5$ = 407.07 $[M]^+$; m/z (Obs.) = 408.21 $[M^+H]^+$.

2.7.4 Ethyl-7-amino-5-(4-methoxyphenyl)-4-oxo-2-thioxo-2, 3, 4, 5-tetrahydro-1H-pyrano[2, 3-*d*]pyrimidine-6-carboxylate (4d)

Light yellow powder; Yield: 97%; m.p.: 224 °C; FT-IR (cm^{-1}): 3682.51, 3218.14(NH), 3064.97,3017.80(CH), 1824.74(C=O), 1581.45, 1477.65(C=C), 1361.24, 1245.96(C=S); ^{1}H-NMR δ(ppm): 2.47 (s, 3H, CH_3), 3.34 (s, 3H, OCH_3), 3.89 (s, 2H, CH_2), 4.27 (s, 1H), 7.03 (m, 2H, ArH), 7.81 (2H, m, ArH), 8.41 (s, br, 2H, NH_2), 9.83 (1H, s, NH), 12.27 (1H, s, NH); ^{13}C NMR δ (ppm): 14.5, 36.8, 56.2, 63.9, 114.5, 116.1, 125.9, 131.5, 133.8, 138.2, 156.5, 160.8, 162.4, 164.5, 168.4, 178.9 ppm LCMS: m/z (Calcd). $C_{17}H_{17}N_3O_5S$ = 374.1270 $[M]^+$; m/z (Obs.) = 374.116.

3. Results and discussion

Herein, we aimed to implement a green protocol to synthesize pyrano[2, 3-*d*]pyrimidine in a fast, simple, efficient, and recyclable manner.

3.1 Preparation & characterization of Fe_3O_4@APTES-SO_3H catalyst

The required core-shell MNPs were prepared using WELFSA and detailed preparation, and further step coating using APTES, followed by SO_3H functionalization (Scheme 1). Raman spectrum collected for final surface synthesized Fe_3O_4@APTES-SO_3H catalyst analysis showed absorption band at 223 cm^{-1} corresponding to the presence of Si-N/Si-O in the core of the catalyst and prominent band at 654 cm^{-1} owing to the presence of or Fe-O in the catalyst. Moreover, the Fe core and its surface modification generate a layer of APTES, and the band at 1113 cm^{-1} confirms the occurrence of the Si-O bond. The band at 1462 cm^{-1} suggests the existence of the surface-SO_3H functionality (Fig. 1).

The X-ray diffraction (XRD) pattern also supported the surface modification. The prominent peak at the 2θ value 15.69° was due to the sulphur. A characteristic peak ob-

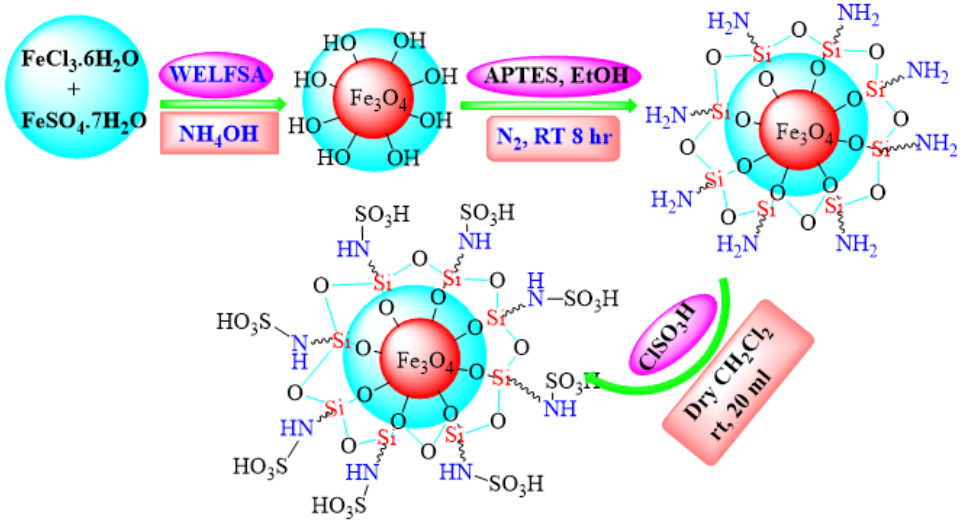

Scheme 1. Preparation of Fe_3O_4@APTES-SO_3H catalyst.

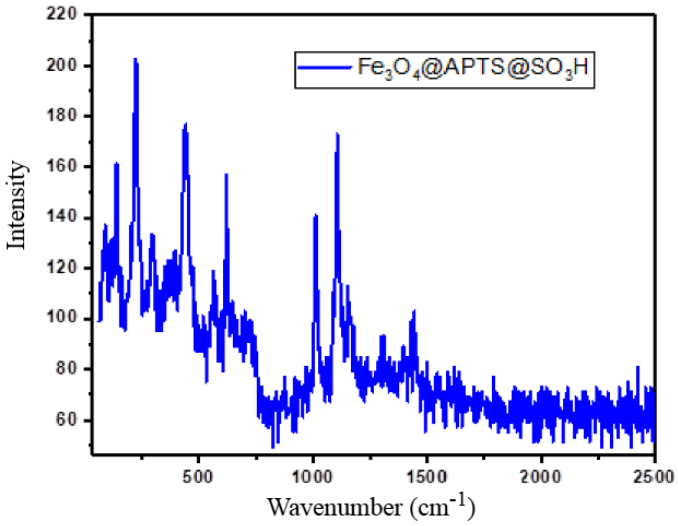

Figure 1. Raman spectrum of Fe_3O_4@APTES-SO_3H.

served at 2θ value 20.11° for the indexed presence of silica. Two other observed peaks at 2θ, 35.72°, 39.91°, 45.74°, 52.73°, 58.09°, 62.98° indicate the presence of Fe_3O_4. The diffractogram of prepared material indicates that the nature is crystalline and Fe_3O_4 data are well compatible with 2θ values of respective Miller indices cubic iron oxide phase with structure of inverse spinel ferrite of magnetite (JCPDS file no.19-0629) [26]. Therefore, the XRD diffractogram of core-shell formation of the catalyst and surface fabrication of Fe_3O_4@APTES-SO_3H gets confirmed (Fig. 2). Further, they are vacuum dried.

Further material was investigated for surface morphology by Field Emission Scanning Electron Microscopy (FE-SEM). It can be observed that the catalyst has retained its crystallinity after surface functionalization (Fig. 3a), with a size of 500 nm. In the SEM image, small grooves caused by -SO_3H functionality are very well visible (Fig. 3b). Finally, the elemental mapping (Fig. 3c) shows the presence and confirmation of elements Fe, O, N, Si & S in the catalyst (Fig. 4). At the same time, Energy Dispersive Spectroscopy (EDS) profile peaks at 0.2, 0.3, 0.35, 0.5, 1.7, 2.4, and 6.4 keV confirmed the elements S, N, O, Fe, Si, and Fe, respectively (Fig. 4).

Investigated the catalytic activity of the synthesized catalyst, for the three-component MCRs of aromatic aldehyde (2 mmol) (1), ethylcyanoacetete (2 mmol) (2), and barbituric acid (2 mmol) (3) in the presence of the catalyst Fe_3O_4@APTES-SO_3H (10 mg) under MWI for 3 – 4 min irradiation at 300 W as model reaction for pyrano[2, 3-*d*]pyrimidine derivative synthesis. The progress of the reaction was observed by TLC. The reaction mixture was diluted with hot ethanol, and the catalyst was separated using a strong external magnet. The ethanol fraction was collected and concentrated to minimum amount, and recrystallized at cold temperature to isolate pure product.

Catalyst integrity

The structural integrity of the Fe_3O_4@APTES-SO_3H catalyst was finally assessed by TEM and XRD. In this purpose, 3-Aminopropyl triethoxysilane was conducted in ethanol for 45 min under H_2 with 10 mol % of Fe_3O_4@APTES-SO_3H NPs. The powder, partially aggregated at the bottom of the autoclave, was recovered after reaction by centrifu-

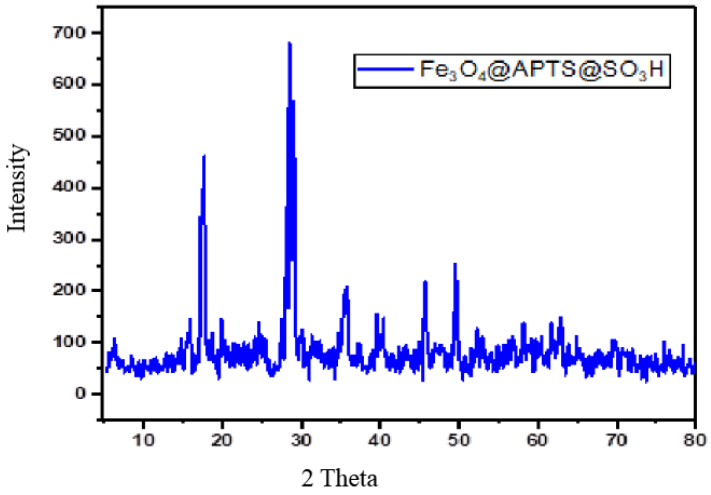

Figure 2. XRD profile of Fe_3O_4@APTES-SO_3H.

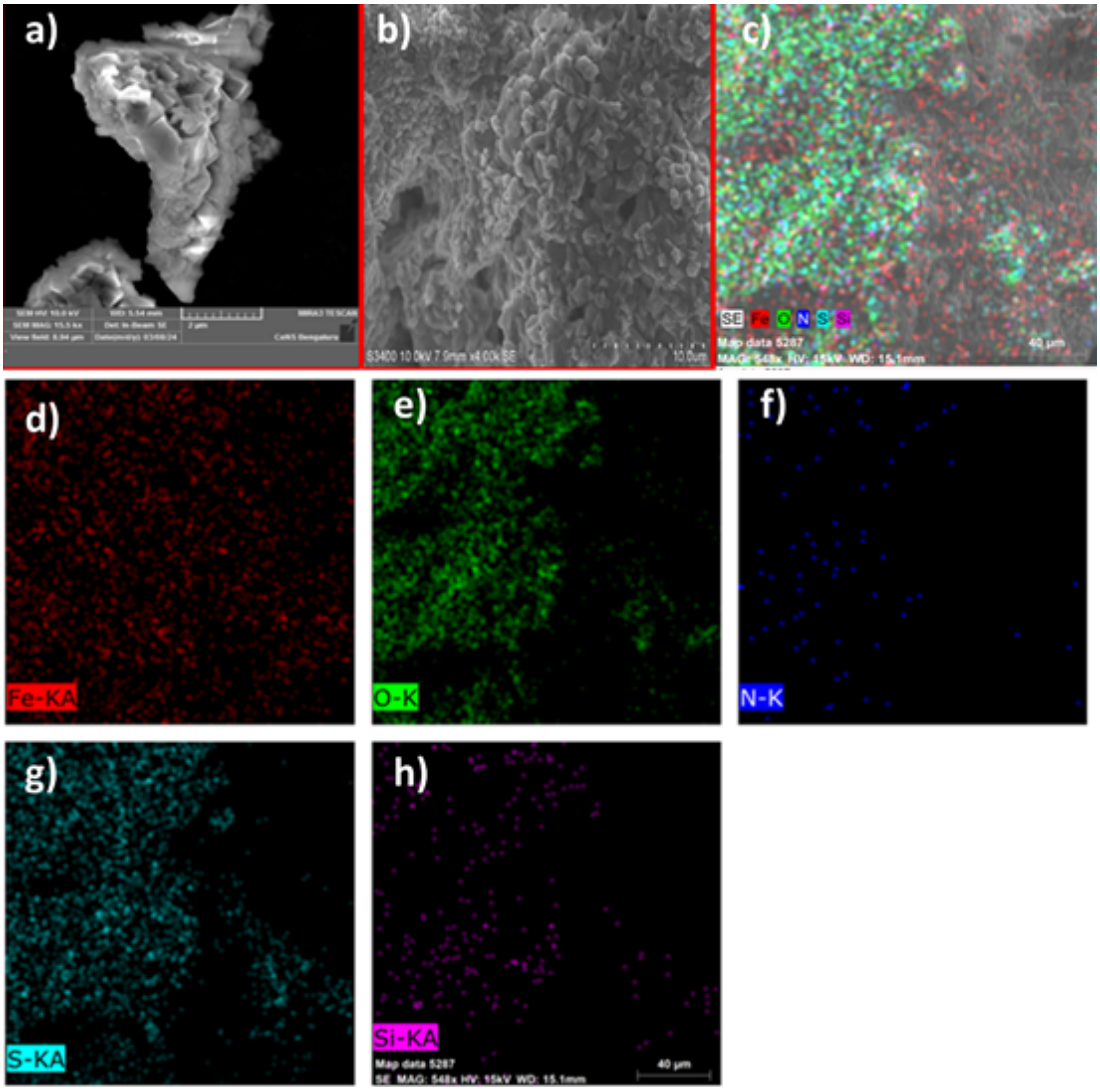

Figure 3. FE-SEM of fabricated catalysts (a & b), and elemental mapping (c-h).

gation and dried under a flux of N_2. Electronic microscopy confirmed that the morphology of the NPs has not changed and there seems to be no degradation of the surface (Fig. 5).

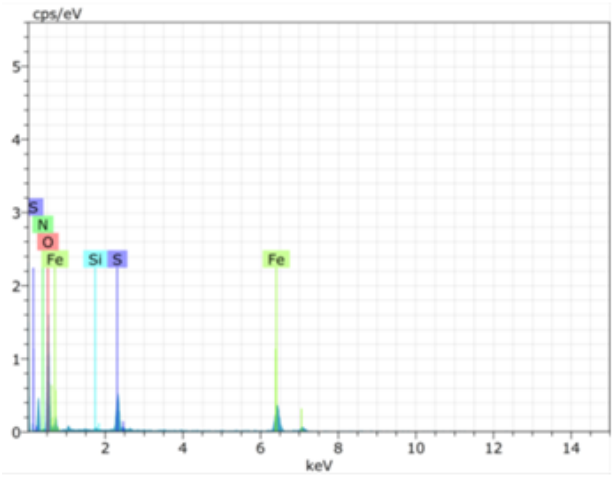

Figure 4. EDS profile of Fe_3O_4@APTES-SO_3H.

3.2 Optimization of reaction

We have proposed here in solid-supported synthesis of fused pyrano[2, 3-*d*]pyrimidine derivatives (Scheme 2) triggered by heterogeneous catalysts (Fe_3O_4@APTES-SO_3H) for the reaction of benzaldehyde (1), ethyl cyanoacetate (2), and barbituric acid or thiobarbituric acid (**3**) in 1 mmol scale reaction for optimizing amount of catalysis required.

A series of reactions containing different quantities of catalysts 0, 2, 4, 6, 8, 10, and 12 mg under MWI 300 W energy were performed and results are tabulated in (Table 1). The catalyst used was from 2 to 10 mg and a gradual increasing of product yield was observed (entries 2 – 6, Table 1). But in case of 12 mg catalyst isolated product yield showed no changes as of 10 mg. The reaction was also conducted in the absence of the catalyst; but surprised to see no product isolation (entry 1). The optimization reaction showed that for 1 mmol of the reaction, we needed a catalyst of 10 mg, 300 W power for 5 min irradiation (entry 6, Table 1). Further increasing the amount of the catalysts, no change was observed in the isolation of the product, or decrease in the reaction time.

Further to optimize different microwave energy suitable

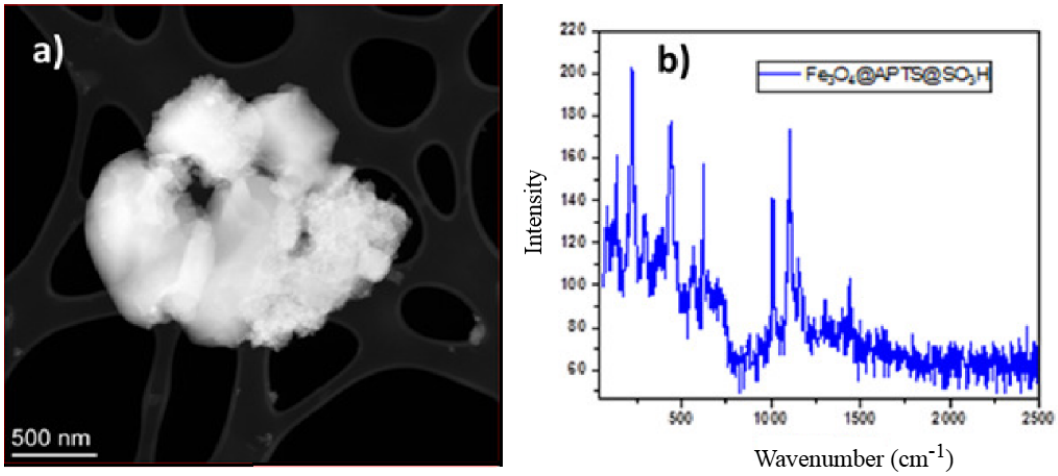

Figure 5. Structural integrity of the catalyst (a) TEM image and (b) X–Ray Diffractogram of Fe_3O_4@APTES-SO_3H NPs.

for the reaction, reaction starting from 100, 180, 300, 450 and 600 W were evaluated (entries 4 – 8, Table 2). This optimization study showed us that 300 W is the perfect irradiation power for this reaction, granting a good separation of the product in only 5 min irradiation time. In order to obtain improved method for the synthesis of pyrano[2, 3-*d*]pyrimidine, model reaction in optimized reaction condition was performed by other methods such as grindstone method, ultrasonic irradiation, rt stirring and MWI (entries 1 – 3, Table 2). These experiments proved that under mechano-chemical method using the pestle-mortar isolated only 30% of the product after 60 min of grinding on/off reaction. The ultrasonic irradiation for 60 min gave only 60% products. However, reaction at 25 °C by stirring gave only 40% isolation yield, even after stirring 2 h (Table 2). Overall this optimization reaction suggested 10 mg of catalyst, 300 W MWI for 5 min is required to achieve better yield.

Additionally, the substrate scope of the existing method for various Electron Donating Group (EDG) and Electron Withdrawing Group (EWG) that were on the aryl aldehyde produced pyrano[2, 3-*d*]pyrimidine. The results for the isolated products are given in Table 3. Isolated product yield varied interestingly less for both EDG and EWG in the aromatic aldehyde substitution, i.e., no significant difference in isolation of the product yield noted. This study highlights that virtually no substitution effect during product formation was noticed when utilizing these optimized catalysts

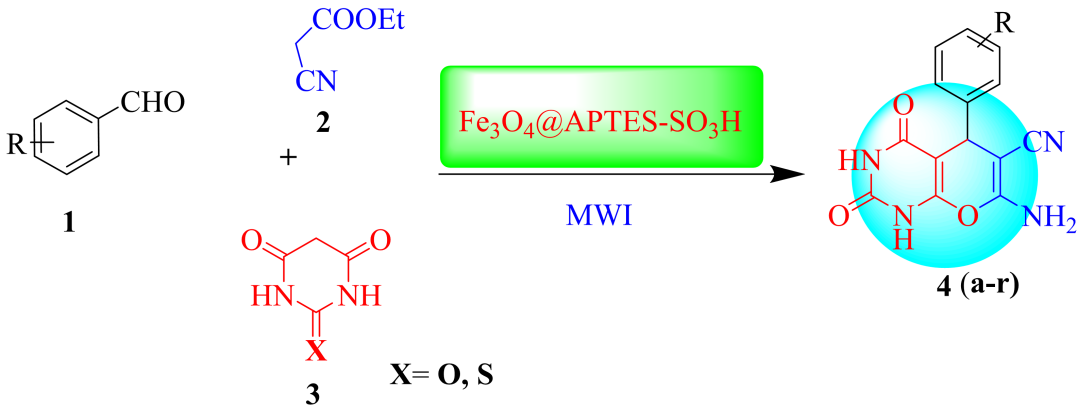

Scheme 2. General synthesis of pyrano[2, 3-*d*]pyrimidine derivative.

Table 1. Catalyst optimization.

Entry	Catalyst (mg)	Time (min)	Yield (%)
1	0	12	-
2	2	5	38
3	4	5	49
4	6	5	71
5	8	5	80
6	10	5	92
7	12	5	92

Table 2. Optimization of the method & MW power.

Entry	Methods	MW power (W)	Time (min)	Yield (%)
1	Mechanochemical grinding	-	60	30
2	Ultrasonication	-	60	60
3	Room temperature stirring	-	120	40
4	MWI	100	5	32
5	MWI	180	5	41
6	**MWI**	**300**	**5**	**92**
7	MWI	450	5	90
8	MWI	600	5	90

Table 3. Pyrano[2, 3-*d*]pyrimidines: reactant and product structure with physical properties.

Entry	Aldehyde	Barbituric acid	Product	Yield (%)	m.p. (°C) Obs./Lit.
1	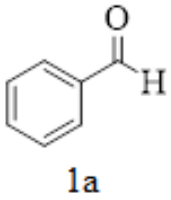 1a	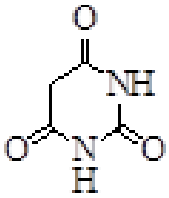	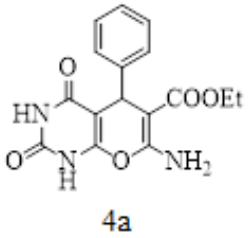 4a	92	208/ New
2	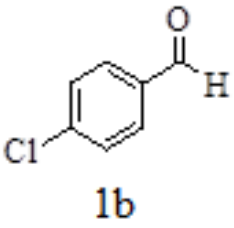 1b	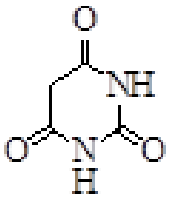	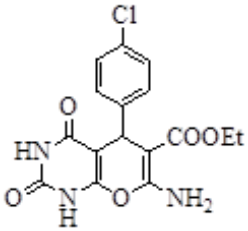 4b	89	282/ New
3	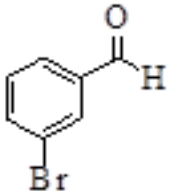 1c	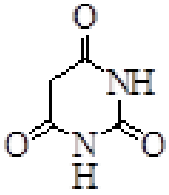	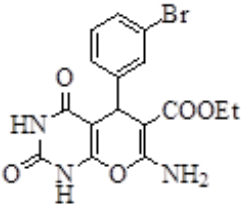 4c	91	235/ New
4	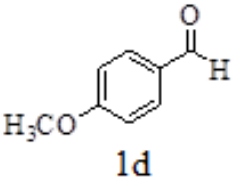 1d	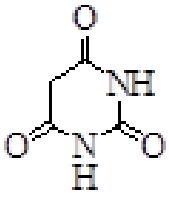	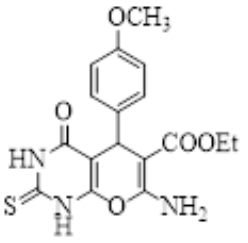 4d	86	224/ New

Continued of Table 3.

Entry	Aldehyde	Barbituric acid	Product	Yield (%)	m.p. (°C) Obs./Lit.
5	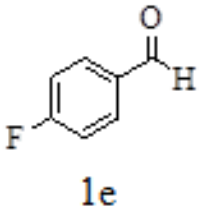 1e	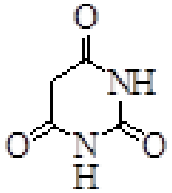	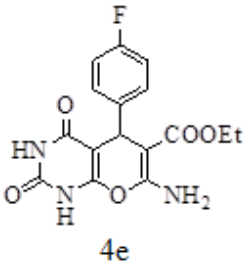 4e	84	225/ 222 – 224 [16]
6	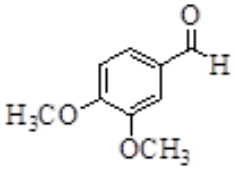 1f	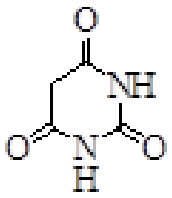	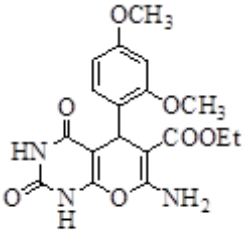 4f	89	295/ 293 – 29 [17]
7	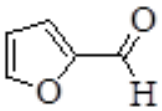 1g	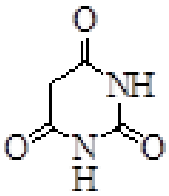	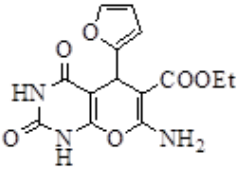 4g	83	259/ 257 – 258 [18]
8	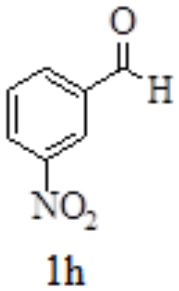 1h	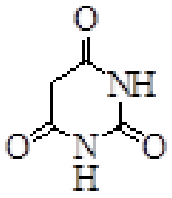	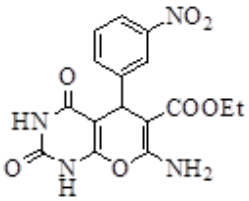 4h	88	260/ 262 – 264 [19]
9	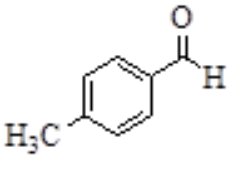 1i	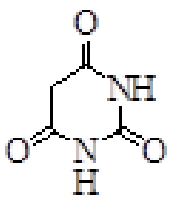	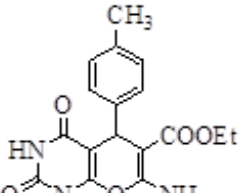 4i	82	297/ 295 – 297 [20]

Continued of Table 3.

Entry	Aldehyde	Barbituric acid	Product	Yield (%)	m.p. (°C) Obs./Lit.
10	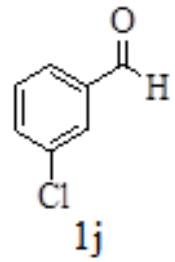 1j	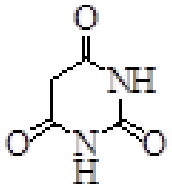	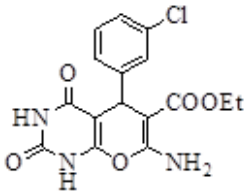 4j	92	280/ 282 – 284 [21]
11	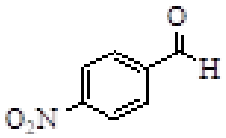 1k	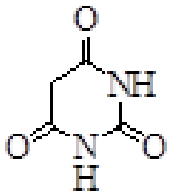	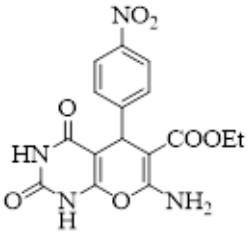 4k	90	293/ 295 – 297 [22]
12	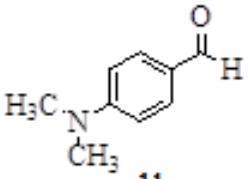 1l	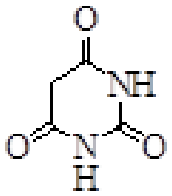	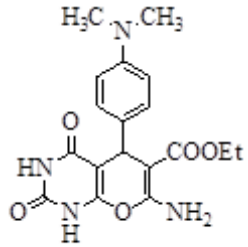 4l	87	285/ 284 – 285 [23]
13	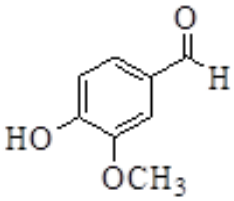 1m	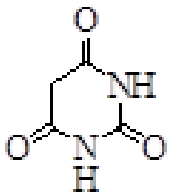	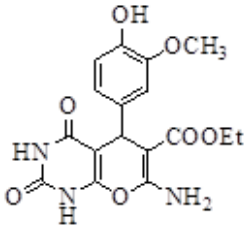 4m	90	172/ 172 – 174 [24]
14	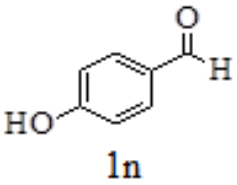 1n	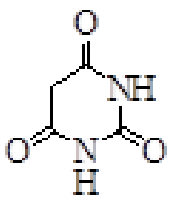	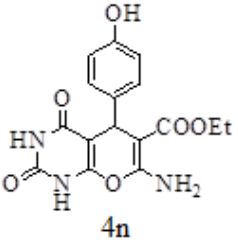 4n	89	168/ 169 – 171 [25]

Continued of Table 3.

Entry	Aldehyde	Barbituric acid	Product	Yield (%)	m.p. (°C) Obs./Lit.
15	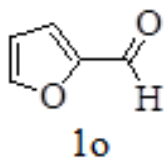 1o	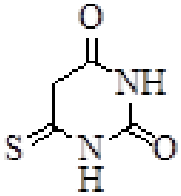	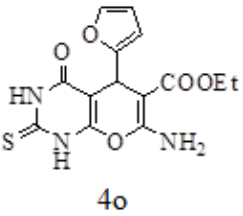 4o	86	235/ 233 – 234 [26]
16	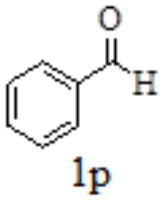 1p	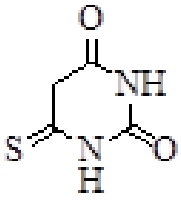	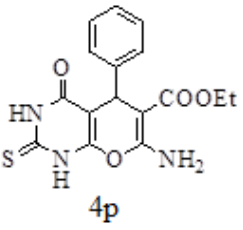 4p	82	220/ 218 – 219 [27]
17	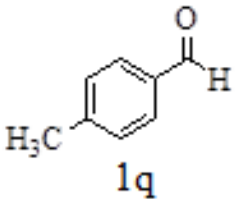 1q	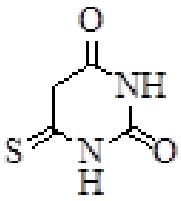	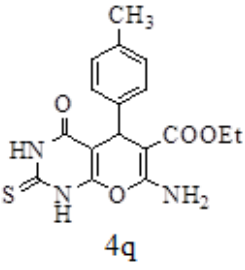 4q	88	211/ 209 – 210 [28]
18	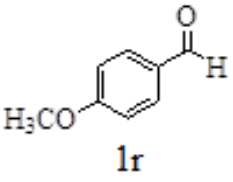 1r	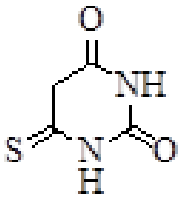	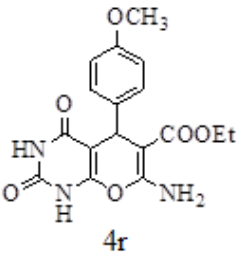 4r	89	224/ 223 – 224 [29]

and reaction conditions.

3.3 Discussion of present approach vs literature methods

We also compared the current green method with selected literature reported methods for pyrano[2, 3-*d*]pyrimidine synthesis (Table 4). Reported reaction and catalyst in (Table 4 entries 1 – 13), some of these methods utilize costly catalysts and extreme conditions, organic solvents that are hazardous to the environment (Table 4 entries no.2, 4, 5, 6, 9, 11, and 12), long time, and low yield. The present protocol reaction developed an eco-friendly approach, simple and efficient for the synthesis of pyrano[2, 3-c]pyrazoles scaffolds.

3.4 Possible mechanism of pyrano[2, 3-*d*]pyrimidine derivatives

The mechanism for the synthesis of pyrano[2, 3-*d*]pyrimidine derivative from aryl aldehyde (1), ethyl cyanoacetate (2), and barbituric or thiobarbituric acid (3a)

Table 4. Comparison of the present method and the reported.

Entry	Catalyst	Condition	Time (min)	Yield (%) [Ref.]
1	MNP@AVOPc	rt/Solvent free	15	94 [30]
2	Fe_3O_4@MSN-FA	80 °C / H_2O	180 – 190	70 [31]
3	MNPs@Cu	Solvent free	8	95 [32]
4	Fe_3O_4@ SPION	Ball Milling/rt	240 – 260	73 [33]
5	γ-Fe_2O_3@DEG	Reflux/ EtOH	120 – 180	69 [34]
6	Fe_3O_4@SiO_2@SBA-15	Solvent free	300 – 360	77 [35]
7	SPION@SiO_2	H_2O	30	91 [36]
8	Fe_3O_4@Ala	Hexane, DCM,	60	94 [36]
9	Fe_3O_4@IONRs	Solvent free	300 – 480	60 [37]
10	$AuFe_3O_4$@GSH	Solvent free	15 – 30	85 [38]
11	$NiFe_2O_4$	EtOH	60 – 80	58 [39]
12	Fe_3O_4@SiO_2@OA	EtOH	120	80 [40]
13	**Fe_3O_4@APTES@SO_3H**	**MW/EtOH**	**5**	**92**

using Fe_3O_4@APTES@SO_3H catalyst is illustrated in (Scheme 3). The first step is Knoevenagel condensation in which the aromatic aldehyde (1) reacts with ethyl cyanoacetate (2) in the presence of catalysts forming ethyl 2-cyano-3-arylacrylate (2a), which in turn gives the intermediate (3b) by reacting with barbituric or thiobarbituric acid (3), give intermediate (3c) due to its tautomerization, and cyclized forming intermediate (3d) due to nucleophilic attack of the -OH group with -CN moiety. Finally undergoes a 1,3-proton transfer and gives the target pyrano[2, 3-*d*]pyrimidine product (4).

3.5 Reusability of the catalysts

The reusability of the catalyst in the synthesis of pyrano[2, 3-*d*]pyrimidine derivative using a model reaction was studied. The isolated product yields for the cycles 1 to 5 were 92%, 90%, 85%, 80%, and 75%, respectively, and a total product isolation loss of 13% was detected over the 5 runs recycled reactions (Fig. 6). As shown by these recycling studies, the catalyst could be easily separated from an external magnet.

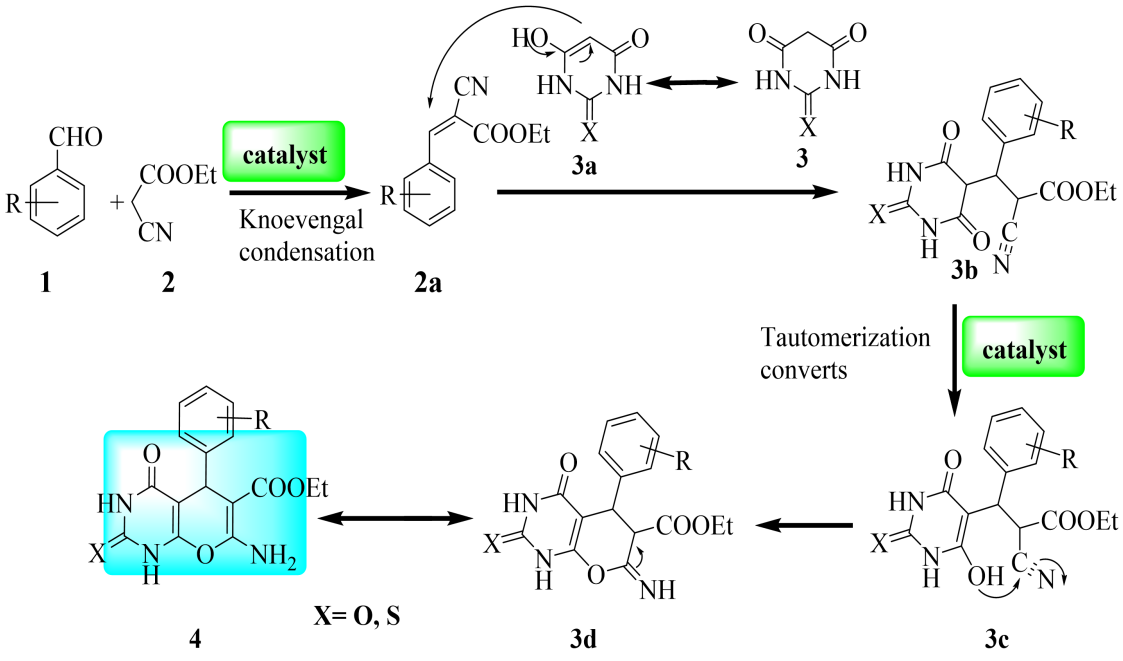

Scheme 3. Possible mechanisms for the formation of pyrano [2, 3-*d*]pyrimidine.

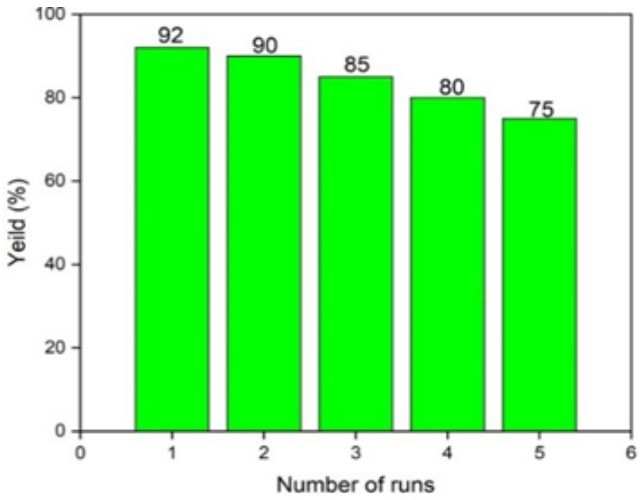

Figure 6. Reusability of the catalysts.

Also, it only needed small quantity for the reaction and can be reused for 4 cycles, producing little waste.
Turnover frequency (TOF) and turnover number (TON) values for the catalysts and recycled for up to 5 run were calculated. Both the numbers decrease in each cycle due to loss of the active site or poisoning. The TOF and TON values were summarized in Table 5.

3.6 Evaluation of the biological activities

To test the antimicrobial activities of a few selected pyrano[2, 3-*d*]pyrimidine derivatives (4a, 4d, 4o, and 4r) employing the standard disk-diffusion method of the Clinical and Laboratory Standards Institute [41]. The in vitro antimicrobial inhibition assay was performed by employing the agar media disc method at 37 °C. The data presented showed that all of the compounds possess biological activity against the labels *Candida albicans* and *Aspergillus niger* fungi. Bacterial and fungal activity was tested against the compounds, with the best performance seen for 4a, 4d, and 4r. Among them, the derivatives of 4o exhibited strong inhibitory effects on Pseduomonas aeruginosa-italicize, while 4f and 4m showed the most significant activity against *Candida*. Derivatives 4a and 4r displayed the highest activity against *A.niger* The presence of heterocycles containing oxygen, nitrogen and sulphur heteroatom are responsible for this high antimicrobial activity. Table 6 shows the detailed antibacterial and antifungal activities of the tested compounds.

4. Conclusion

This work has explored the preparation method of iron oxide-SO_3H that influenced the Lewis acid catalyst approach by bio-throwing and reported method. Moreover, we demonstrated the usage of the synthesized catalysts for the synthesis of pyrano[2, 3-*d*]pyrimidine derivatives through one-pot three-component MCRs of aryl aldehyde, ethyl cyanoacetate, and barbituric acid in one step, catalysed by Fe_3O_4@APTES-SO_3H, a novel heterogeneous catalyst. The novelty in this method is agro-waste based solvent medium used in core shell iron oxide preparation and then its surface functionalization with silica and sulphonic acid moiety. Various techniques are applied to characterize the prepared catalysts. The method developed is rapid, simple to isolate the product, cheap, recyclable, and a green protocol for the synthesis of valuable heterocyclic compounds. The FT-IR, ^{1}H-NMR, ^{13}C-NMR, and LC-MS methods were used to characterize all the synthesized compounds. A disc diffusion method was performed to evaluate the additional antimicrobial activities of selected pyrano[2, 3-*d*]pyrimidines (4a, 4d, and 4f), and these derivatives exhibited moderate activities compared to standard drugs as a reference.

Acknowledgement
The authors are thankful to the SERB-SURE, GOI, and RCU-IDR-2022-23 for the financial support to Dr. K.K.

Supplementary information
FT-IR, ^{1}H-, ^{13}C-NMR and LC-MS of the selected compounds are available in supplementary.

Table 5. Calculation of TON & TOF of the catalysts recycle.

	RUN 1	RUN 2	RUN 3	RUN 3	RUN 4	RUN 5
TON	136.1	134.6	130.1	128.3	125.4	124.8
TOF	9.1	8.8	8.4	6.5	5.6	4.9

Table 6. antimicrobial activity (antibacterial & antifungal).

	Organisms	Compounds	75 μL/ mL	50 μL/mL	25 μL/mL	10 μL/mL	5 μL/mL
Antibacterial activity	***B. subtilis***	4a	21 mm	18 mm	12 mm	R	R
		4d	19 mm	15 mm	12 mm	R	R
		4f	13 mm	R	R	R	R
		4m	14 mm	R	R	R	R
		4o	11 mm	12 mm	R	R	R
		4r	13 mm	10 mm	R	R	R
	Ciprofloxacin		-	-	-	**30** mm	**35** mm
	E. coli	4a	13 mm	R	R	R	R
		4d	11 mm	10 mm	R	R	R
		4f	11 mm	R	R	R	R
		4m	11 mm	R	R	R	R
		4o	21 mm	10 mm	R	R	R
		4r	13 mm	R	R	R	R
	Ciprofloxacin		-	-	-	-	**25** mm
	P. aeruginosa	4a	13 mm	R	R	R	R
		4d	16 mm	10 mm	R	R	R
		4f	14 mm	10 mm	R	R	R
		4m	13 mm	10 mm	R	R	R
		4o	19 mm	13 mm	R	R	R
		4r	11 mm	R	R	R	R
	Ciprofloxacin		-	-	**45** mm	-	-
Antifungal activity	***C. albicans***	4a	12 mm	10 mm	R	R	R
		4d	20 mm	15 mm	R	R	R
		4f	18 mm	15 mm	13 mm	R	R
		4m	28 mm	25 mm	13 mm	R	R
		4o	25 mm	20 mm	R	R	R
		4r	10 mm	R	R	R	R
	Fluconazole		-	-	**30** mm	-	-
	A. niger	4a	18 mm	15 mm	10 mm	R	R
		4d	13 mm	12 mm	R	R	R
		4f	15 mm	10 mm	R	R	R
		4m	12 mm	R	R	R	R
		4o	10 mm	R	R	R	R
		4r	15 mm	10 mm	R	R	R
	Fluconazole		-	-	**23** mm	-	-

Authors contributions
Authors have equally contributed in acquisition and analysing the data as well as preparing the paper.

Availability of data and materials
The data that support the findings of this study are available from the corresponding author, upon reasonable request.

Conflict of interests
The author declare that they have no known competing financial interests or personal relationships that could have appeared to influence the work reported in this paper.

Abbreviations

^{13}C-NMR	: ^{13}Carbon-nuclear magnetic resonance
^{1}H-NMR	: Proton-nuclear magnetic resonance
APTES	:(3-Aminopropyl) triethoxysilane
DCM	: Dichloromethane
Fe_3O_4	: Iron (III) oxide
$FeCl_3$	: Iron (III) chloride
FT-IR	: Fourier transform infrared spectroscopy
gm	: Gram
HCl	: Hydrochloric acid
J	: Coupling constant
mg	: Milligram
mmol	: Millimolar
mL	: Milliliter
VSM	: Vibrating sample magnetometer
WELFSA	: Water extract of lemon fruit shell ash
XRD	: X-ray diffraction
dd	: double distilled water
rt	:Room temperature

References

[1] P. Panahi, N. Nouruzi, E. Doustkhah, H. Mohtasham, A. Ahadi, A. Ghiasi-Moaser, S. Rostamnia, G. Mahmoudi, and A. Khataee. *Ultrason. Sonochem*, **58**(2019):104653–104672. DOI: https://doi.org/10.1016/j.ultsonch.2023.106540.

[2] M. Piltan. *Heterocycl. Comm.*, **23**(2017):401–425, . DOI: https://doi.org/10.1016/j.trac.2019.06.007.

[3] M. Saraei, N. Valizadeh, and H. Ebrahimi-asl. *Monatsh. Chem.*, **146**(2015):345–357. DOI: https://doi.org/10.1037/fsh0000119.

[4] D. Azarifar, H. Ebrahimiasl, R. Karamian, and M. Ahmadi-Khoei. *J. Iran. Chem. Soc.*, **16**(2019):341–354. DOI: https://doi.org/10.1007/s40266-019-00640-5.

[5] H. Ebrahimiasl, D. Azarifar, M. Mohammadi, and H. Keypour. *Res. Chem. Intermed.*, **47**(2020):683–687. DOI: https://doi.org/10.1038/sj.eye.6703103.

[6] S. Rostamnia, E. Doustkhah, A. Baghban, and B. Zeynizadeh. *J. Appl. Polym. Sci.*, **133**(2016):1–53. DOI: https://doi.org/10.1080/00031305.2016.1154108.

[7] E. Doustkhah, S. Rostamnia, and A. Hassankhani. *J. Porous Mater.*, **23**(2016):549–565, . DOI: https://doi.org/10.1038/nature14131.

[8] I. A. Ibarra, A. Islas-Jácome, and E. González-Zamora. *Org. Biomol. Chem.*, **16**(2018):1402–1425. DOI: https://doi.org/10.1039/C70B02305G.

[9] R. Tahawy, E. Doustkhah, E. S. A. Abdel-Aal, M. Esmat, F. E. Farghaly, H. El-Hosainy, N. Tsunoji, F. I. El-Hosiny, Y. Yamauchi, M. H. N. Assadi, and Y. Ide. *Appl. Catal. B: Environ.*, **286**(2021): 119854–119863. DOI: https://doi.org/10.1016/j.jclepro.2019.05.103.

[10] S. S. Mofarah, L. Schreck, C. Cazorla, X. Zheng, E. Adabifiroozjaei, C. Tsounis, J. Scott, R. Shahmiri, Y. Yao, R. Abbasi, and Y. Wang. *Nanoscale*, **13**(2021):6764–6779. DOI: https://doi.org/10.3390/ijms22136764.

[11] E. Doustkhah, R. Hassandoost, A. Khataee, R. Luque, and M. H. N. Assadi. *Chem. Soc. Rev.*, **50**(2021):2927–2939, . DOI: https://doi.org/10.1021/acssuschemeng.2c00645.

[12] T. S. Rad, Z. Ansarian, A. Khataee, B. Vahid, and E. Doustkhah. *Sep. Purif. Technol.*, **256**(2021):117811–117835. DOI: https://doi.org/10.1016/j.seppur.2020.117811.

[13] A. Zebardasti, M. G. Dekamin, E. Doustkhah, and M. H. N. Assadi. *Inorg. Chem.*, **59**(2020):11223–11239. DOI: https://doi.org/10.1016/j.heliyon.2023.e16315.

[14] E. Doustkhah, H. Mohtasham, M. Farajzadeh, S. Rostamnia, Y. Wang, H. Arandiyan, and M. H. N. Assadi. *Micropor. Mesopor. Mat.*, **293**(2020):109832–109843, . DOI: https://doi.org/10.1039/D2RA06888E.

[15] M. Aalinejad, N. N. Pesyan, and E. Doustkhah. *Mol. Catal.*, **494**(2020):111117–111189. DOI: https://doi.org/10.1002/cctc.202300643.

[16] E. Doustkhah, H. Mohtasham, M. Hasani, Y. Ide, S. Rostamnia, N. Tsunoji, and M. H. N. Assadi. *Mol. Catal.*, **482**(2020):110676–110689, . DOI: https://doi.org/10.1002/slct.202000813.

[17] J. Li, Y. F. Zhao, X. Y. Yuan, J. X. Xu, and P. Gong. *Molecules*, **11**(2006):574. DOI: https://doi.org/10.3390/11070574.

[18] S. S. Karbasaki, G. Bagherzade, B. Maleki, and M. Ghani. *J. Taiwan Inst. Chem. Eng.*, **118**(2021):342–365. DOI: https://doi.org/10.1016/j.jtice.2020.12.025.

[19] B. Maleki, R. Nejat, H. Alinezhad, S. M. Mousavi, B. Mahdavi, and M. Delavari. *Org. Prep. Proced. Int.*, **52**(2020):328–339. DOI: https://doi.org/10.1080/00304948.2020.1765655.

[20] B. Maleki. *Org. Prep. Proced. Int.*, **48**(2016):303–343. DOI: https://doi.org/10.1021/acssuschemeng.4c02659.

[21] R. Tayebee, M. Jomei, B. Maleki, M. K. Razi, H. Veisi, and M. Bakherad. *J. Mol. Liq.*, **206**(2015):119–129. DOI: https://doi.org/10.2174/1385272827666230124145625.

[22] R. W. Carling, K. W. Moore, L. J. Street, D. Wild, C. Isted, P. D. Leeson, S. Thomas, D. O'Connor, R. M. McKernan, K. Quirk, S. M. Cook, J. R. Atack, K. A. Wafford, S. A. Thompson, G. R. Dawson, P. Ferris, and J. L. Castro. *J. Med. Chem.*, **47**(2004):1807–1827. DOI: https://doi.org/10.1016/j.bmc.2010.11.050.

[23] M. A. Shaikh, M. Farooqui, and S. Abed. *Res. Chem. Intermed.*, **44**(2018):5483–96. DOI: https://doi.org/10.1039/D3RA00049D.

[24] S. Grasso, G. De Sarro, A. De Sarro, N. Micale, M. Zappala, G. Puja, M. Baraldi, and C. De Micheli. *J. Med. Chem.*, **43**(2000):2851–2869. DOI: https://doi.org/10.1021/jm991086d.

[25] E. Doustkhah, A. Baghban, M. H. N. Assadi, R. Luque, and S. Rostamnia. *Catal. Lett.*, **149**(2019):591–600, . DOI: https://doi.org/10.1039/D4OB01589D.

[26] Y. A. Tayade and D. S. Dalal. *Catal. Lett.*, **147**(2017):1411–1426. DOI: https://doi.org/10.1007/s10562-017-2032-6.

[27] A. V. Chatea, P. K. Bhadkea, M. A. Khandea, J. N. Sangshettib, and C. H. Gill. *Chin. Chem. Lett.*, **28**(2017):1577–1587. DOI: https://doi.org/10.1016/j.cclet.2017.03.007.

[28] D. C. Mungra, M. P. Patel, D. P. Rajani, and R. G. Patel. *Eur. J. Med. Chem.*, **46**(2011):4192–4225. DOI: https://doi.org/10.1016/j.ejmech.2011.06.022.

[29] M. Kidwai, S. Saxena, M. K. R. Khan, and S. S. Thukral. *Bioorg. Med. Chem. Lett.*, **15**(2005):4295–4315. DOI: https://doi.org/10.1016/j.bmcl.2005.06.041.

[30] Y. C. Wu, W. F. Fong, J. X. Zhang, C. H. Leung, H. L. Kwong, M. S. Yang, D. Li, and H. Y. Cheung. *Eur. J. Pharmacol*, **473**(2003):9–43. DOI: https://doi.org/10.1016/j.rechem.2024.101530.

[31] L. Bonsignorel, G. Loyl, D. Seccil, and A. Calignanoz. *Eur. J. Med. Chem.*, **28**(1993):517–576. DOI: https://doi.org/10.1016/0223-5234(93)90020-F.

[32] S. Patil, A. Mane, and S. Dhongade-Desai. *J. Iran. Chem. Soc.*, **16**(2019):1665–1675.
DOI: https://doi.org/10.1007/s13738-019-01640-3.

[33] A. El Hallaoui, S. Chehab, B. Malek, O. Zimou, T. Ghailane, S. Boukhris, A. Souizi, and R. Ghailane. *ChemistrySelect*, **4**(2019): 3062–3163.
DOI: https://doi.org/10.1002/slct.202204635.

[34] H. Sharma and S. Srivastava. *RSC Adv.*, **8**(2018):38974–38985.
DOI: https://doi.org/10.1039/C8RA06889E.

[35] H. Ebrahimiasl and D. Azarifar. *Appl. Organomet. Chem.*, **34**(2019): 5359–5378.
DOI: https://doi.org/10.1002/aoc.5359.

[36] U. C. R. Divya and D. S. Rawat. *RSC Adv.*, **4**(2014):41323–41569.
DOI: https://doi.org/10.1039/C4RA06803C.

[37] M. Tajbakhsh, M. Farhang, R. Hosseinzadeh, and Y. Sarrafi. *RSC Adv.*, **4**(2014):23116–23216.
DOI: https://doi.org/10.1039/C4RA03333G.

[38] J. Safaei-Ghomi, H. Shahbazi-Alavi, A. Ziarati, R. Teymuri, and M. R. Saberi. *Chin. Chem. Lett.*, **25**(2014):401–426.
DOI: https://doi.org/10.1016/j.cclet.2013.11.046.

[39] R. Ghahremanzadeh, G. I. Shakibaei, and A. Bazgir. *Synlett.*, **8**(2008):1129–1149.
DOI: https://doi.org/10.1055/s-2008-1072716.

[40] M. R. Nabid, S. J. T. Rezaei, R. Ghahremanzadeh, and A. Bazgir. *Ultrason. Sonochem*, **17**(2010):159–179.
DOI: https://doi.org/10.1016/j.ultsonch.2009.06.012.

[41] M. Piltan. *Heterocycl. Commun.*, **23**(2017):401–403, .
DOI: https://doi.org/10.1515/hc-2017-0142.